J|A|C|S
ARTICLES
Published on Web 12/08/2006

Changeover during in Situ Compositional Modulation of Hexacyanoferrate (Prussian Blue) Material

Paulo Roberto Bueno,[†] David Giménez-Romero,[‡] Claude Gabrielli,*[,‡] José Juan García-Jareño,[§] Hubert Perrot,[‡] and Francisco Vicente[§]

Contribution from the Instituto de Química, Departamento de Físico-Química, Universidade Estadual Paulista, P.O. Box 355, 14801-907, Araraquara, São Paulo, Brazil, UPR 15 du CNRS, Laboratoire Interface et Système Electrochimique, 4 place Jussieu, 75252 Paris, France, and Departament de Química Física, Universitat de València, C/ Dr Moliner, 50, 46100, Burjassot, València, Spain

Received October 2, 2006; E-mail: cg@ccr.jussieu.fr

Abstract: This paper describes the importance of $(H_2O)_6$ clusters in controlling the properties of hexacyanoferrate (Prussian Blue) materials. A careful in situ study of compositional changes by using electrogravimetric techniques (in ac and dc modes) in hexacyanoferrates containing K^+ alkali metals reveals the existence of a changeover in the properties of these films in a narrow potential range. Control of the compositional variation of the changeover is dependent on the K^+ stoichiometric number in the compound structure. However, a specific K^+ occupation in the compound structure activates the occupation of the $(H_2O)_6$ cluster by H_3O^+ and/or H^+, causing the changeover in the properties of hexacyanoferrate film. Thus, the information thus obtained is very useful for understanding the mechanisms involved in the electrochemical reversible switch between ferrimagnetism/paramagnetism, "semiconductor/metal" and electroluminescence/nonelectroluminescence properties of molecular cyanide materials.

Introduction

Materials in which identical metal atoms exist in different spin and/or oxidation states, often referred to as mixed valence materials, are of particular interest for applications in magnetic, electronic, and optical fields.[1−7] Within this class of materials, a particular type is based on molecular entities with unpaired electron spins residing in d- or f-orbitals. Ensembles of these molecules form a solid structured 3D network in which spins reside in orbitals (d or f) of the individual metallic entities.[7,8] Therefore, the electronic or magnetic state of the metal atoms at particular sites can be tailored by external conditions, e.g., magnetic field,[9−13] pressure, light,[1,9−15] and/or by changes in a specific local crystal environment (e.g., due to electrochemical compositional in situ variation[1,2,8,16−19]).

A typical example is Prussian Blue (PB) material and its analogues.[1,8] In PB materials, iron metal centers exist in either low- or high-spin configurations, depending on whether metal atoms reside on the carbon or nitrogen side of the cyanide ligands ($Fe_k^{3+}-NC-Fe_l^{2+}$, in which k and l refer to the site occupancy in the general formula, which will be presented later herein).[20] The nitrogen and cyanide ligands are responsible for holding the material together, as a solid 3D structure (see Figure 1), forming fcc structures in which the metal atoms centers are octahedrally surrounded by N and C atoms.[13,20]

Recently, many PB analogues have been shown to exhibit interesting (even extraordinary) magnetic,[4] optical,[1,10,14] and electrochemical properties[1,8,19,21−23] and also a great potential

[†] Universidade Estadual Paulista.
[‡] UPR 15 du CNRS.
[§] Universitat de València.

(1) Sato, O.; Iyoda, T.; Fujishima, A.; Hashimoto, K. *Science* **1996**, *271*, 49−51.
(2) Garcia-Jareno, J. J.; Gimenez-Romero, D.; Vicente, F.; Gabrielli, C.; Keddam, M.; Perrot, H. *J. Phys. Chem. B* **2003**, *107* (41), 11321−11330.
(3) Mortimer, R. J.; Reynolds, J. R. *J. Mater. Chem.* **2005**, *15* (22), 2226−2233.
(4) Sato, O.; Iyoda, T.; Fujishima, A.; Hashimoto, K. *Science* **1996**, *272* (5262), 704−705.
(5) Sato, O.; Einaga, Y.; Iyoda, T.; Fujishima, A.; Hashimoto, K. *J. Electrochem. Soc.* **1997**, *144* (1), L11−L13.
(6) Sato, O.; Hayami, S.; Einaga, Y.; Gu, Z. Z. *Bull. Chem. Soc. Jpn.* **2003**, *76* (3), 443−470.
(7) Gu, Z. Z.; Sato, O.; Iyoda, T.; Hashimoto, K.; Fujishima, A. *Chem. Mater.* **1997**, *9* (5), 1092−1097.
(8) de Tacconi, N. R.; Rajeshwar, K.; Lezna, R. O. *Chem. Mater.* **2003**, *15* (16), 3046−3062.
(9) Hayami, S.; Gu, Z.-Z.; Shiro, M.; Einaga, Y.; Fujishima, A.; Sato, O. *J. Am. Chem. Soc.* **2000**, *122*, 7126−7127.
(10) Sato, O.; Einaga, Y.; Fujishima, A.; Hashimoto, K. *Inorg. Chem.* **1999**, *38* (20), 4405−4412.
(11) Yamamoto, T.; Umemura, Y.; Sato, O.; Einaga, Y. *J. Am. Chem. Soc.* **2005**, *127* (46), 16065−16073.
(12) Champion, G.; Escax, V.; Moulin, C. C. D.; Bleuzen, A.; Villain, F. O.; Baudelet, F.; Dartyge, E.; Verdaguer, N. *J. Am. Chem. Soc.* **2001**, *123* (50), 12544−12546.
(13) Kumar, A.; Yusuf, S. M.; Keller, L. *Phys. Rev. B* **2005**, *71* (5).
(14) Sato, O. *J. Photochem. Photobiol., C* **2004**, *5* (3), 203−223.
(15) Sato, O.; Kawakami, T.; Kimura, M.; Hishiya, S.; Kubo, S.; Einaga, Y. *J. Am. Chem. Soc.* **2004**, *126* (41), 13176−13177.
(16) Gabrielli, C.; Garcia-Jareno, J. J.; Keddam, M.; Perrot, H.; Vicente, F. *J. Phys. Chem. B* **2002**, *106* (12), 3182−3191.
(17) Gimenez-Romero, D.; Bueno, P. R.; Garcia-Jareno, J. J.; Gabrielli, C.; Perrot, H.; Vicente, F. *J. Phys. Chem. B* **2006**, *110*, 2715−2722.
(18) de Tacconi, N. R.; Rajeshwar, K.; Lezna, R. O. *J. Electroanal. Chem.* **2006**, *587* (1), 42−55.
(19) Itaya, K.; Akahoshi, H.; Toshima, S. *J. Electrochem. Soc.* **1982**, *129*, 1498.
(20) Herren, F.; Fischer, P.; Ludi, A.; Halg, W. *Inorg. Chem.* **1980**, *19*, 956.
(21) Neff, V. D. J. *J. Electrochem. Soc.* **1978**, *125*, 886.
(22) Feldman, B. J.; Murray, R. W. *Anal. Chem.* **1986,** *58*, 2844.
(23) Kuleska, P. J.; Galus, Z. *Electrochim. Acta.* **1997**, *42*, 867.

10.1021/ja066982a CCC: $33.50

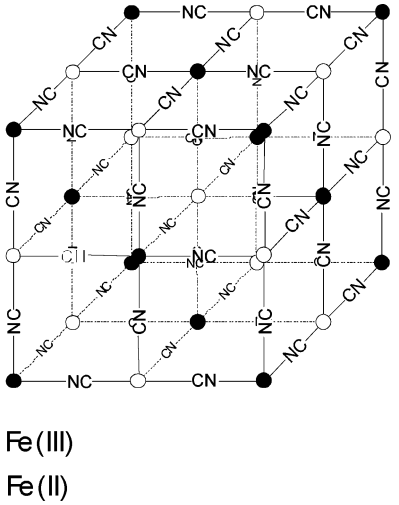

Figure 1. Structure of Prussian Blue hexacyanoferrates. It is believed that the vacancies in the $Fe'(CN)_6$ site are surrounded by water molecules ($Fe'(CN)_{6-m}m(H_2O)$ sites), whose stoichiometry is very difficult to be determined. Interstitial alkali metals were omitted for clarity.

for device applications (e.g., molecular magnets,[24] nanowires,[25−28] rechargeable battery devices). These technologically desirable properties of PB materials are directly linked to the detailed periodic arrangement of the bridged metal centers.[24]

PB is the historical name of an ancient pigment which is recognized today as belonging to a very important family of functional inorganic materials: traditional hexacyanometallate materials (indeed, PB pertains to the subclass called hexacyanoferrates), which are represented by the general M'_k $[M''(CN)_6]_l \cdot mH_2O$ formula in which M′ and M″ are the 3d transition metal (iron in the PB structure).[13,20] In the periodic structure, M′ is generally ascribed to the high spin metallic site (Fe^{3+}) and M″ to the low spin site (Fe^{2+}). The Fe^{2+} metallic site is surrounded by carbon octahedra, and the strong ligand field is considered as the origin of the low spin configuration. On the other hand, the Fe^{3+} metallic site is surrounded by nitrogen octahedra and the moderate or weak ligand field is considered to be as the origin of the high-spin configuration.[13,20]

The electronic and spin states of hexacyanometallates containing an alkali metal (e.g., Na^+, K^+, etc.) strongly depend on the atomic composition ratio of Fe^{3+}/Fe^{2+}, so that different high and low magnetic sites can exist and the number of such sites can be designed according to the alkali metal composition. In other words, the hexacyanometallate crystal structure tolerates different electronic spins limiting the super-exchange interactions to those across CN bridges, thus allowing tunneling of magnetism and coloration.[1,4−12,14,15,24,25,27−30] Furthermore, elaborated theoretical analyses suggest that the local disorder plays an important role in determining the photomagnetic properties. Experimental studies as a function of chemical composition have shown that structural defects, namely $\{Fe(CN)_6\}$ vacancies filled by $\{(H_2O)_6\}$ clusters, are a prerequisite for photomagnetism.[29,31] In other words, much more attention must be given to the water part considered in the general formula, since it is likely linked to the local disorder existing in the structure.[17,20,29,31−34]

Water molecules, in this case, occupy the interstitial positions. Therefore, for $k/l = 1$, the first coordination shell of Fe^{3+} and Fe^{2+} are $\{Fe^{3+}(NC)_6\}$ and $\{Fe^{2+}(CN)_6\}$, respectively. When $k/l > 1$ in the general formula, some of the vacancies are filled by water molecules (or clusters), and ideally, the first coordinations of Fe^{3+} and Fe^{2+} are, respectively, $\{Fe^{3+}(NC)_{6-m}m(H_2O)\}$ and $\{Fe^{2+}(CN)_6\}$. In the latter case, i.e., when $k/l > 1$, there are two types of water molecules: (i) water molecules coordinated to Fe^{3+} octahedral in empty nitrogen sites and (ii) uncoordinated water molecules in interstitial positions.[13,20]

It has recently been shown that the ionic exchange of an alkali metal, i.e., K^+, is dependent on the water-hydrated crystalline part of the PB structure.[17] The amount of the water-hydrated crystalline part of the structure has been stated to be environmentally dependent, making it very difficult to pinpoint the water's chemical composition in the general formula, regardless of the preparation methodologies employed.[13,20] Indeed, special methodologies that take this aspect into account must be developed. In this paper, an electrogravimetric technique (in dc and ac modes) will be used to investigate the role of this water-hydrated crystalline part and to describe the existence of a changeover in the properties controlled by a characteristic compositional variation in a narrow potential range.

The unique structural arrangement of hexacyanometallate materials and its route for compositional variations lead to a combination of properties, besides magnetic properties, which are not readily found in any other inorganic material. One of these properties is optical absorbance, which stems from a strong charge-transfer band that occurs between the transition metal centers. The modulation of this valence can easily be done electrochemically, leading to significant optical absorbance shifts.[1,8,24] This electrochemical control is traditionally recognized as an in situ metal alkali compositional change, so that the atomic composition ratio of Fe^{3+}/Fe^{2+} varies according to the electrochemical potential and different high and low magnetic sites exist and can change together with absorbance shifts.[1,8,14,24]

However, it is important to keep in mind that, according to detailed studies involving monitoring of the electrochemical and mass variations, the ionic compensation of the Fe^{3+}/Fe^{2+} ratio variation is given not only by K^+ compositional changes but also by changes in the composition of the crystalline structure of water molecules.[8,17,31]

In Prussian Blue materials containing K^+ alkali metals having the general formula $K_hFe_k[Fe(CN)_6]_l \cdot mH_2O$, i.e., hexacyanoferrates containing K^+, the modulation of the Fe^{3+}/Fe^{2+} ratio can be described as follows:[17]

(24) Sato, O. *Acc. Chem. Res.* **2003,** *36*, 692−700.
(25) Ishii, S.; Sadki, E. S.; Ooi, S.; Ochiai, Y.; Hirata, K. *Physica C* **2005**, *426*, 268−272.
(26) Palmino, F.; Ehret, E.; Mansour, L.; Duverger, E.; Labrune, J. C. *Surf. Sci.* **2005**, *586* (1−3), 56−64.
(27) Zhang, X. Y.; Dai, J. Y. *Nanotechnology* **2004**, *15* (9), 1166−1168.
(28) Ji, G. B.; Tang, S. L.; Gu, B. X.; Du, Y. W. *J. Phys. Chem. B* **2004**, *108* (26), 8862−8865.
(29) Goujon, A.; Varret, F.; Escax, V.; Bleuzen, A. V. M. *Polyhedron* **2001**, *20*, 1339.
(30) Yokoyama, T.; Ohta, T.; Sato, O.; Hashimoto, K. *Phys. Rev. B* **1998**, *58* (13), 8257−8266.
(31) Bleuzen, A.; Lomenech, C.; Escax, V.; Villain, F.; Varret, F.; Cartier dit Moulin, C.; Verdaguer, M. *J. Am. Chem. Soc.* **2000**, *122*, 6648.
(32) Gimenez-Romero, D.; Bueno, P. R.; Garcia-Jareno, J. J.; Gabrielli, C.; Perrot, H.; Vicente, F. *J. Phys. Chem. B* **2006**, *110*, 19364.
(33) Gimenez-Romero, D.; Bueno, P. R.; Garcia-Jareno, J. J.; Gabrielli, C.; Perrot, H.; Vicente, F. *J. Phys. Chem. B* **2006**, *110*, 19352.
(34) Buser, H. J.; Shwazenbach, D.; Petter, W.; Ludi, A. *Inorg. Chem.* **1977**, *16*, 2704.

$$K_hFe_k[Fe(CN)_6]_l{\cdot}mH_2O + nK^+_{electrolyte} + ne^- \rightleftarrows K_{h+n}Fe_{k-n}Fe_n[Fe(CN)_6]_l{\cdot}mH_2O \quad (1)$$

$$K_hFe_k[Fe(CN)_6]_l{\cdot}mH_2O(nOH^-) + nH^+_{electrolyte} + ne^- \rightleftarrows K_hFe_{k-n}Fe_n[Fe(CN)_6]_l{\cdot}mH_2O(nH_2O) \quad (2)$$

$$K_hFe_k[Fe(CN)_6]_l{\cdot}mH_2O + nH_3O^+_{electrolyte} + ne^- \rightleftarrows K_hFe_{k-n}Fe_n[Fe(CN)_6]_l{\cdot}mH_2O(nH_3O^+) \quad (3)$$

When a potential change occurs, ions are exchanged between the material and the solution to compensate for the charge lost or gained by the material. This leads to a potential-controlled compositional variation, and during this compositional variation with respect to the K^+ insertion, eq 1, the PB, $K_hFe_k[Fe(CN)_6]_l{\cdot}mH_2O$, is reversibly converted to $K_{h+n}Fe_{k-n}Fe_n[Fe(CN)_6]_l{\cdot}mH_2O$, known as Everitt's Salt (ES). Thus, the amount of K^+ can be controlled by an ne^- modulation and hence by the potential.

Considering the three-dimensional cubic framework and the Fe^{3+}/Fe^{2+} ratio variation, it is difficult to differentiate between the likely distinct electronic sites during an in situ compositional variation, according to the mechanism of eqs 1 to 3. As it can be seen, all of them lead to $Fe'_k{-}NC{-}Fe''_l$, so that a variation in the $Fe^{+3}{}_k/Fe^{+2}{}_l$ ratio can be controlled by ne^- changes imposed by the electrochemical potential.[17] Then, it is difficult to directly separate the compositional variations due to the metal alkali K^+ or H^+ and/or H_3O^+, the last two related to the crystalline part of water molecules. However, thanks to modern electrogravimetric techniques (exploited in ac and dc modes),[1,2,16,17,32,33,35] the processes can be fully separated and the compositional variations in $Fe^{3+}(CN)_{6-m}m(H_2O)$ sites, kinetically linked to optical and magnetic properties, can be studied in detail by following the in situ magnetic and optical variations as a function of the composition.

By starting to explore the possibilities given by this mechanism, the goal of this paper is to demonstrate a changeover that occurs during the electrochemical composition modulation of K^+. The changeover here will be shown to occur at a specific compositional point. As mentioned earlier, the compositional variations modulate the electric/optic (and perhaps magnetic) properties of hexacyanoferrate materials; this is a very important aspect of the material to be explored further.

Experimental Section

The compositional changes in response to an electrochemical modulation were carried out in a typical electrochemical three-electrode cell. The $K_hFe_k[Fe(CN)_6]_l{\cdot}mH_2O$ hexacyanoferrates were deposited on 25 mm^2 diameter gold electrodes of a quartz crystal (6 MHz, CQE Troyes, France) inserted in a fast-response microbalance. A platinum grid was used as the counter electrode, and a Saturated Calomel Electrode (SCE) was used as the reference electrode. The compositional variations were modulated by controlled changes in the charge and mass of $K_hFe_k[Fe(CN)_6]_l{\cdot}mH_2O$ by means of an AUTOLAB potentiostat-galvanostat (PGSTAT100). The electrolyte used in all the experiments was 0.25 M KCl (A.R., R.P. NORMAPURTM) with a controlled pH of about 2.23.[2,17,35]

The compositional variation due to mass changes of the $K_hFe_k[Fe(CN)_6]_l{\cdot}mH_2O$ hexacyanoferrate was carried out simultaneously to the charge variation applied by a homemade Electrochemical Quartz Crystal Microbalance (EQCM, homemade − CNRS, France) coupled to the potentiostat-galvanostat. The $K_hFe_k[Fe(CN)_6]_l{\cdot}mH_2O$ hexacyanoferrate deposit was sufficiently thin to ensure a precise relationship between the frequency variation of the quartz crystal and the mass change without any viscoelastic artifacts. Details are given in refs 2, 17, 32, 33, and 35.

To monitor the compositional variation of $K_hFe_k[Fe(CN)_6]_l{\cdot}mH_2O$ due to K^+ changes, the EQCM, operating in the ac mode, was coupled to electrochemical impedance spectroscopy. This technique is referred to in literature as ac-electrogravimetry, and details of the technique and methodology of separation of the processes involved in eqs 1 to 3 are given by specific references.[32,33] The frequency response measurements were fulfilled in the frequency interval from 0.01 to 6×10^4 Hz. The ac experiments were initially stabilized during 60 s at the steady-state potential and realized with a potential modulation amplitude of 50 mV rms.

The$K_hFe_k[Fe(CN)_6]_l{\cdot}mH_2O$ was electrochemically deposited on one of the gold electrodes of a quartz crystal in 0.02 M $K_3Fe(CN)_6$ (A.R., R.P. NORMAPURTM), 0.02 M $FeCl_3$ (A.R., R.P. NORMAPURTM), and 0.01 M HCl (A.R., R.P. NORMAPURTM) solution. A controlled cathodic current of 40 μA cm^{-2} was applied for 150 s to obtain $Fe_4[Fe(CN)_6]_3{\cdot}mH_2O$. After this deposition, the $K_hFe_k[Fe(CN)_6]_l{\cdot}mH_2O$ was obtained by cycling in the [0.6, −0.25] V potential range in 0.25 M KCl with a controlled pH of 2.23, according to refs 2, 3, 17, and 35−37.

Results

Kinetic Aspects. (i) Electrogravimetry − DC Mode. Figure 2a shows the voltammetric scan and mass change of the $K_hFe_k[Fe(CN)_6]_l{\cdot}mH_2O$ material, previously stabilized in the electrolytic environment in which the measurements were carried out. The stabilization process is very important, as explained in refs 2,3,17, and 35−37 because $K_hFe_k[Fe(CN)_6]_l{\cdot}mH_2O$ is obtained and synthesized through this process.

$K_hFe_k[Fe(CN)_6]_l{\cdot}mH_2O$ is commonly referred to as soluble PB, and during a compositional variation with respect to the K^+ insertion, eq 1, the soluble PB is reversibly converted to $K_{h+n}Fe_{k-n}Fe_n[Fe(CN)_6]_l{\cdot}mH_2O$, known as Everitt's Salt (ES). The amount of K^+ can be controlled by ne^- modulations. The mass change combined with the charge was monitored by means of the $F(dm/dQ)$ function, which represents the instantaneous ratio between the mass change and the ne^- imposed by the electrochemical potential. A negative value of this function means the exchange of cations between the electrolyte and the $K_{h+n}Fe_k[Fe(CN)_6]_l{\cdot}mH_2O$ host, e.g., K^+, H^+, or H_3O^+, in the present case.[17] In addition, the analysis of $F(dm/dQ)$ provides information on the molecular weight as a function of ne^- variation. Thus, the compositional changes as a function of the imposed electrochemical potential can be completely monitored.

At this point, it is very important to emphasize that $K_{h+n}Fe_{k-n}Fe_n[Fe(CN)_6]_l{\cdot}mH_2O$ differs from $K_hFe_k[Fe(CN)_6]_l{\cdot}mH_2O$ only by the Fe'_k/Fe''_l ratio and the occupation of the K^+ sites. However, this difference has profound implications in the material's physical and chemical properties. This aspect has been extensively discussed and studied in the literature.[2,17,21,32,33,35,38] Note, also, that the Fe'_k/Fe''_l ratio, at least ideally, is lower than the initial value as a function of K^+ insertion due to the conversion of Fe'_k into Fe''_n, according to eq 1 and in the same proportion of the ne^- variation. In Figure 2a, the potentiostatic

(35) Garcia-Jareno, J. J.; Gabrielli, C.; Perrot, H. *Electrochem. Commun.* **2000**, *2* (3), 195−200.
(36) Kellawi, H.; Rosseinsky, D. R. J. *J. Electroanal. Chem.* **1982**, *131*, 373.
(37) Rosseinsky, D. R. J.; Glasser, L.; Jenkins, H. D. B. J. *J. Am. Chem. Soc.* **2004**, *126*, 10472.
(38) Lundgren, C. A.; Murray, R. W. *Inorg. Chem.* **1988**, *27*, 933.

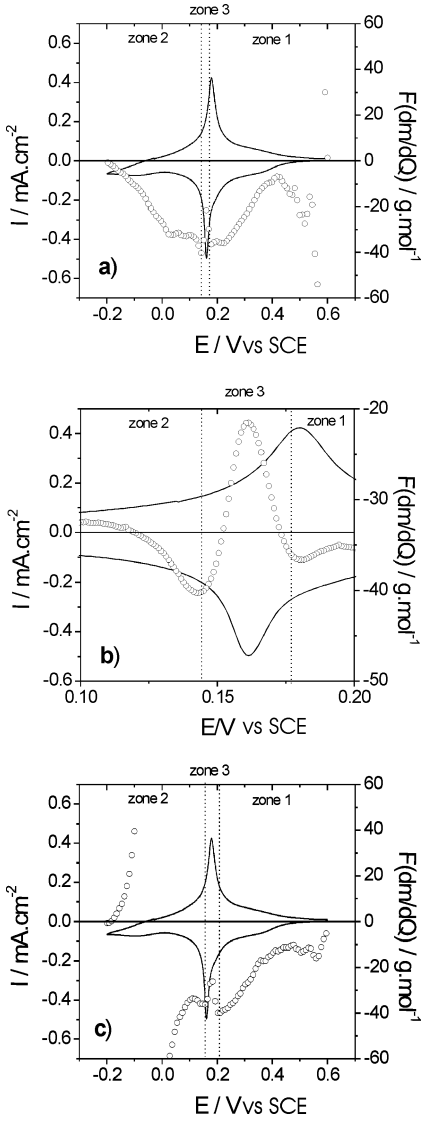

Figure 2. Voltammetric scan (solid line) and (●) $F(\mathrm{d}m/\mathrm{d}Q)$ function of $K_hFe_k[Fe(CN)_6]_l \cdot mH_2O$ material, previously stabilized in the electrolytic environment. The electrolyte was 0.25 M KCl in a pH of about 2.23. (a) $F(\mathrm{d}m/\mathrm{d}Q)$ function here is represented during the cathodic compositional variation (insertion); (b) zoom of zone 3 of (a) and (c) $F(\mathrm{d}m/\mathrm{d}Q)$ function represented during the anodic compositional variation (deinsertion).

scan is cyclical, which means that the insertion and deinsertion of K^+ occurs and there are two peaks, one anodic and the other cathodic (redox peaks). However, for clarity, the mass change, $F(\mathrm{d}m/\mathrm{d}Q)$, was plotted in Figure 2 only during the ionic insertion.

Also for clarity, Figure 2a is divided into three distinct regions. The entire voltammetric pattern has already been shown in literature,[17] and its interpretation with respect to the mechanism of eq 1 to 3 has been discussed in detail. Therefore, only the processes regarding zone 3, which have not been detailed so far, are considered. They involve several important aspects related to the properties of hexacyanoferrate materials as a function of the in situ compositional variation. In this region, clearly illustrated in Figure 2b, where the potentials are plotted in a narrower range, the $F(\mathrm{d}m/\mathrm{d}Q)$ increases up to a maximum value. Figure 2a indicates that, in zone 2, from 0.22 V to the beginning of zone 3, the $F(\mathrm{d}m/\mathrm{d}Q)$ function reaches a minimum value of about -39 g mol^{-1}. From this value one can infer that the compositional variation of the material around this potential is mainly due to the compositional variation of K^+ , as stated by most papers in the literature.[2,16,22]

However, from an in-depth analysis of the $F(\mathrm{d}m/\mathrm{d}Q)$ values, given in Figure 2b, it is possible to observe an increase in the $F(\mathrm{d}m/\mathrm{d}Q)$ values in the narrower portion of the peak, corresponding to the potential range from 0.17 V up to 0.14 V, i.e., a difference of only 30 mV. The $F(\mathrm{d}m/\mathrm{d}Q)$ function reaches a maximum exactly at the maximum value of the peak current density and then steadily decreases to the initial values of about -39 g mol^{-1}, when the K^+ compositional variation predominates once more. This behavior may only be related to a decrease in compositional variation due to the K^+ alkali metal to the detriment of other ionic species with a lower molecular weight. A similar behavior is also observed in anodic scans, as illustrated in Figure 2c (the discrepancies between these behaviors are due only to limitations in calculation of the $F(\mathrm{d}m/\mathrm{d}Q)$ function values since this function cannot be defined when current ($\mathrm{d}Q/\mathrm{d}t$) reaches null values).

Now, it is important to mention that the redox peaks observed in the voltammogram (Figure 2a), from 0.3 to 0.1 V, disappear when the alkali metal is absent from the electrolyte. This also occurs even for aqueous electrolytes when H^+ and/or H_3O^+ are present,[17] which are the other species exchanged by the PB during this potential interval. This behavior is explained by the fact that H^+ and/or H_3O^+ cannot occupy the alkali metal sites. The water crystalline part of hexacyanoferrates occupies mainly sites related to the hydrated water part (in the coordinate and uncoordinated water clusters) and cannot substitute K^+ in its site. Accordingly, there is no redox peak when hexacyanoferrate materials cannot be compositionally varied through occupation of the alkali metal sites, due to the absence of this alkali metal in the electrolyte. This fact leads to the conclusion that the compositional variation of K^+ is very important for the main redox process illustrated in Figure 2 and, further, that it cannot exist without a compositional variation of the alkali metal.

Experiments carried out in nonaqueous media by Lupu et al.[39] have shown that there is not any process in the same potential range when there is no K^+ alkali metal in the media (see Figure 1 of ref 39). However, when the experiment is conducted in nonaqueous media in the presence of the K^+ alkali metal, the peak intensity decreased in comparison to the same experiment conducted in an aqueous media. The authors[39] ascribed this decrease to a lower K^+ exchange rate in the nonaqueous media compared to the aqueous electrolyte, attributed especially to the lower solubility of the salt containing potassium. A careful analysis reveals that, if the peak in the range of 0.17 to 0.14 V were suppressed from Figure 2, a similar pattern as that obtained by Lupu et al.[39] in the nonaqueous media would appear. Therefore, this result corroborates the fact that H^+ and/or H_3O^+ exchanges take place in this potential range, as commented on above. On the other hand, this increase of the $F(\mathrm{d}m/\mathrm{d}Q)$ function is not due to the water movement since this movement takes place at more cathodic potentials.[17]

Accordingly, this increment in the peak intensity depends indirectly on the compositional variation of K^+ and arises only when this variation occurs but is not directly involved in the exchange of K^+ with the electrolytic media. In other words, it

(39) Lupu, S.; Mihailciuc, C.; Pigani, L.; Seeber, R.; Totir, N.; Zanardi, C. *Electrochem. Commun.* **2002**, *4* (10), 753−758.

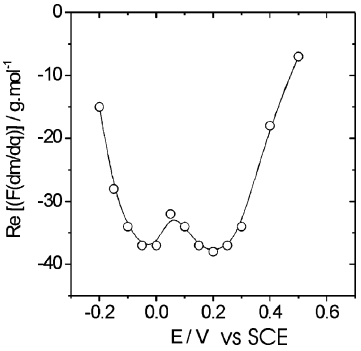

Figure 3. Low-frequency real part of $F(\mathrm{d}m/\mathrm{d}q)$ function obtained by ac electrogravimetry.[33] The experimental conditions were the same as those described under Figure 2 and in the experimental procedure section.

is not related to the mass change of the K^+ compositional variation. It is important to show that this property of the peak is not related with any kinetic effect due to a decrease, for instance, in the K^+ exchange rate, as will be demonstrated in the following section.

(ii) Electrogravimetry − AC Mode. To check this last aspect, it is important to separate the K^+ compositional variation from the other two ionic exchanges, i.e., H^+ and/or H_3O^+ . This separation is only possible thanks to the use of electrogravimetry in the ac mode allied to knowledge of the chemical mechanism described by eqs 1 to 3.[2,16,17,32,33,35] Figure 3 shows the low-frequency value of the $F(\mathrm{d}m/\mathrm{d}Q)$ (i.e., when $\omega \rightarrow 0$) as a function of potential. In this figure, one can see the mass change is due solely to the K^+ exchange, i.e., -39 g mol^{-1}, except in the potential range environ 0.1 V. Consequently, this figure clearly shows that there is an increase in the $F(\mathrm{d}m/\mathrm{d}Q)$ values in the region around 0.1 V, which corresponds to the same region indicated in the results obtained in the non-steady-state measurements shown in Figure 2. It is important to emphasize here that the result illustrated in Figure 3 was obtained in steady-state conditions, so this behavior cannot be explained by kinetic effects. Therefore, this change compensation in this narrow potential range is only due to the exchange of H^+ and/or H_3O^+, the other species exchanged by this material.[17]

The $F(\mathrm{d}m/\mathrm{d}Q)$ changes around these potential values are related to compositional variations in the water crystalline part, i.e., H^+ and/or H_3O^+ (the other species presents into the solution), which can only occur if K^+ increases in the composition of hexacyanoferrate (i.e., zone 3 disappears when K^+ is not present in the electrolyte, as commented on above), reaching certain specific values that activate H^+ and/or H_3O^+ exchanges. This point will be discussed later, since the thermodynamic aspects of K^+ compositional variations before and after the narrow region of potential shown in Figure 2b has to be analyzed first.

Thermodynamic Aspects. The thermodynamics of insertion which leads to a compositional variation in hexacyanoferrate, considering the ionic exchange mechanism of eqs 1 to 3, was developed in ref 32. Therefore, the thermodynamics of the compositional variation of K^+ in hexacyanoferrate will be examined now separately from the other exchange modes of the water crystalline part of the structure.

According to the lattice-gas model, Figure 4 shows the variation of potential as a function of the occupation fraction or compositional variation $y = \eta_k{}^+/N_h$, where $\eta_k{}^+$ is the relative

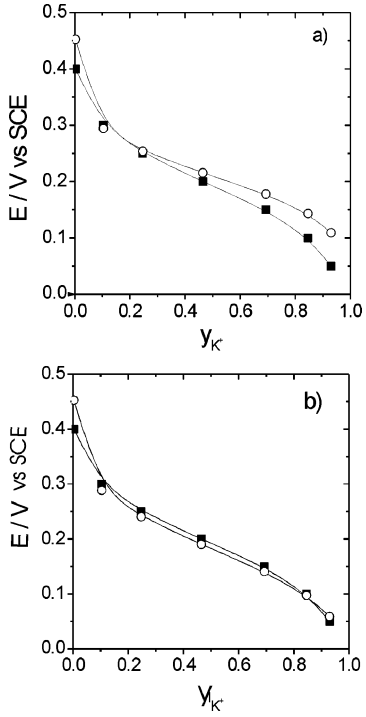

Figure 4. Curve of E versus y_{K^+} under steady-state conditions. The K^+ processes here were separated using ac electrogravimetry[32] carried out in 0.25 M KCl and $T = 298$ K, pH = 2.23. (a) Conditions of nonmean field interactions (eq 4) (simulated values: $eE = 0.45 - k_BT \ln(\{y\}/\{(1-y)\})$) and (b) considering mean field interactions (eq 5) (simulated values: $eE = 0.45 - k_BT \ln(\{y\}/\{(1-y)\}) - 2k_BTy$). (■) Experimental and (○) simulated values.

number density of sites occupied by the K^+ host with respect to the total number density of sites available for K^+ occupation in the host, N_h (details of the separation process and methodologies are given in refs 32 and 33). The pattern in Figure 4 can be adjusted to the following relationship:[32,40]

$$\mu = \Lambda_0 - \epsilon_i k_B T \log[y/(1-y)] \qquad (4)$$

In the above relationship, Λ_0 is the change of Gibbs free energy resulting from the insertion of an isolated ion and electron into the lattice of hexacyanoferrate. In eq 4, ϵ_i is assumed to be -1 for the K^+ compositional variation, according to refs 17 and 33, and μ is the chemical potential of the hexacyanoferrate as a function of y, the density of sites occupied by K^+ in the host, and finally, k_B is the Boltzmann constant. In the present case, μ is related to the potential by $eE = -\mu$, so that E can be plotted with respect to y, as shown in Figure 4.

Figure 4a, specifically, shows a similar relationship between the theoretical and experimental analyses. However, there are some discrepancies starting in a potential range of 0.14−0.20 V. At lower values of the number of inserted K^+ ions in hexacyanoferrates films, the theoretical and experimental analyses are in complete agreement. From the lattice-gas theory for intercalation, it is known that repulsive or attractive interactions are not taken into account in eq 4. To consider repulsive or attractive interactions, a term must be added to eq 4. Here, a mean field interaction was considered,[40] so that

(40) McKinnon, W. R.; Haering, R. R., Modern Aspects of Electrochemistry. In White, R. E.; Bockris, J. O. M.; Conway, B. E. Eds. Plenum Press: New York, **1983**, Vol. *15*, p 235.

$$\mu = \Lambda_0 - \epsilon_i k_B T \log[y/(1-y)] + g k_B T y \qquad (5)$$

in which g is an adimensional interaction parameter that encompasses the interactions between both the intercalated ions and the strain fields caused by the expansion or contraction of the lattice of the inorganic material. The critical value of the interaction parameter is $g = \pm 4$; values outside this range indicate that phase change takes place into the host. Nonetheless, the value of g used in the simulation of Figure 4b is -2. Consequently, there is not a phase change during this potential interval.

Accordingly and taking into account the repulsive term ($g < 0$) considered in the analysis of the experimental pattern (mean field interactions), a good agreement was found between the theoretical and experimental data, according to the results of Figure 4b. Consequently, this means that around the potential range of 0.14−0.20 V, the interactions switch from no interaction to short-range nearest-neighbor repulsive interactions. The latter implies a stepwise change, and K^+ compositional changes become more difficult which is clearly demonstrated in Figure 2b.

Discussion

The kinetic and thermodynamic analyses carried out previously lead to us infer that there is a changeover in this region of potential (zone 3 shown in Figure 2b). Results reported in the literature for the electronic conduction as a function of temperature during compositional variations have shown conclusively that, during compositional variations occurring around the potential range discussed herein, hexacyanoferrates go from a "semiconductive" behavior to a "metal-like" behavior.[41] Accordingly, the changeover pattern can be viewed as a "*continuous*" transition from an "*insulation*" to a "*conduction*" state of the hexacyanoferrates in response to sweeping polarization and compositional changes.

It should be noted that the above discussion also applies to the optical properties. Thus, an optical changeover can also be shown to occur drastically in the potential change of zone 3 (shown in Figure 2b). For instance, luminescence properties change tremendously in this zone of compositional variation.[3] The relative luminescence goes from 35% to 90% during sweeping polarization to large values of h.[3] Moreover, it can be observed that the maximum variation occurs exactly in zone 3.[3]

Finally, it must be emphasized that the aforementioned changeover (estimated from calculations of the electrical charge involved at the beginning of this potential range and the total electrical charge of the process) starts precisely at about 25% of the total electronic transfer. This value is similar to that found for the amount of iron lost during the stabilization of the structure and the formation of $K_hFe_k[Fe(CN)_6]_l{\cdot}mH_2O$[21,38] from the insoluble PB structure and to that value obtained by Goujon et al. for the progressive structural change in PB analogues.[29]

The progressive structural change reported by Goujon et al.[29] in CoFe PB analogue materials takes place in the composition domain of a metal alkali/Co ratio around 0.175−0.53.[42] The structural change causes photoinduced properties when[42,43] the symmetry of the structure goes from face-centered cubic to a tetragonal.

Accordingly and combining all this information to draw a concise picture of the changeover, it can be stated that this picture necessarily involves a more selective entrance of water molecules (H^+ and/or H_3O^+, according to the mechanism of eqs 1 to 3) during the observed changeover, within a potential range of around 0.14−0.17 V. The increase in the $F(dm/dQ)$ values supports this assertion.

Furthermore, during compositional changes, K^+ must preferentially fill sites adjacent to $Fe'(CN)_{6-m}m(H_2O)$ vacancies in the structure that are formed during the $K_hFe_k[Fe(CN)_6]_l{\cdot}mH_2O$ stabilization process. When all these sites are already occupied by a fraction of about 25%, the next possibility is the occupation of the K^+ sites of the structure not adjacent to $Fe'(CN)_{6-m}m(H_2O)$ and, for those types of K^+ sites (where K^+ are used only to reach the film electroneutrality), repulsive interaction exists (see Figure 4). Note here that the situation in which 25% of the charge is exchanged agrees with the ratio found for photoinduced structural conversion.[42,43] This provides strong evidence that the changeover observed in our experiments must involve some structural changes (likely with symmetry changes) similar to that observed in photoinduced experiments,[42,43] and consequently, these changes explain the variations in the electronic structure of these materials within this potential range. Furthermore, these structural changes explain also the entrance of the hydrated proton from this compositional change of K^+ ions.

Accordingly, it can be stated that there are two types of K^+ sites, one of which is preferentially occupied (the one adjacent to $Fe'(CN)_{6-m}m(H_2O)$ vacancies) while the other suffers repulsive interaction (due to structural changes), giving preference (or activating the process) to water molecule sites coordinated to Fe^{3+} octahedral in empty nitrogen sites that are fully or more occupied than initially in the narrow range of potential indicated in Figure 2b.

This is the most probable cause of the changeover that leads to the aforementioned changes in the optical and electrical properties. One can also infer that, in the changeover potential range, when all the K^+ sites become occupied, the compensation of ne^- variation is also activated around the $K^+-Fe'(CN)_{6-m}m(H_2O)$ sites by the variation in the value of m occupation fraction for water clusters. Note that $K^+-Fe'(CN)_{6-m}m(H_2O)$ probably possesses a local charge distribution and energy unlike that of $Fe'(CN)_{6-m}m(H_2O)$, where adjacent potassium ions are absent. Indeed, the previously described feature, combined with the K^+ repulsive interaction, is the reason for the H^+ and/or H_3O^+ selective entrance into the structure to occupy the $m(H_2O)$ sites related to $K-Fe'(CN)_{6-m}m(H_2O)$. The details of the mechanism are sketched in Figure 5. This mechanism explains why it is absolutely necessary for K^+ to be inserted in PB prior to the occurrence of this structural changeover, although the mass changes are not directly related to this ion exchange during in situ compositional variations of hexacyanoferrates in this potential range.

As mentioned in the introduction, it was shown that structural defects such as $\{Fe(CN)_6\}$ vacancies filled by $\{(H_2O)_6\}$ clusters are decisive in defining the photomagnetism properties of hexacyanometallates; hence, the water crystalline part of the structure is crucial to understand the photomagnetism[42,43] and

(41) Garcia-Jareno, J. J.; Sanamatias, A.; Navarro-Laboulais, J.; Benito, D.; Vicente, F. *Electrochemica. Acta.* **1998**, *43*, 235.

(42) Escax, V.; Moulin, C. C. D.; Villain, F.; Champion, G.; Itié, J. P.; Münsch, P.; Verdaguer, M.; Bleuzen, A. C. R. *Chimie* **2003**, *6*, 1165.

(43) Ohkoshi, S. I.; Tokoro, H.; Hashimoto, K. *Coord. Chem. Rev.* **2005**, *249*, 1830.

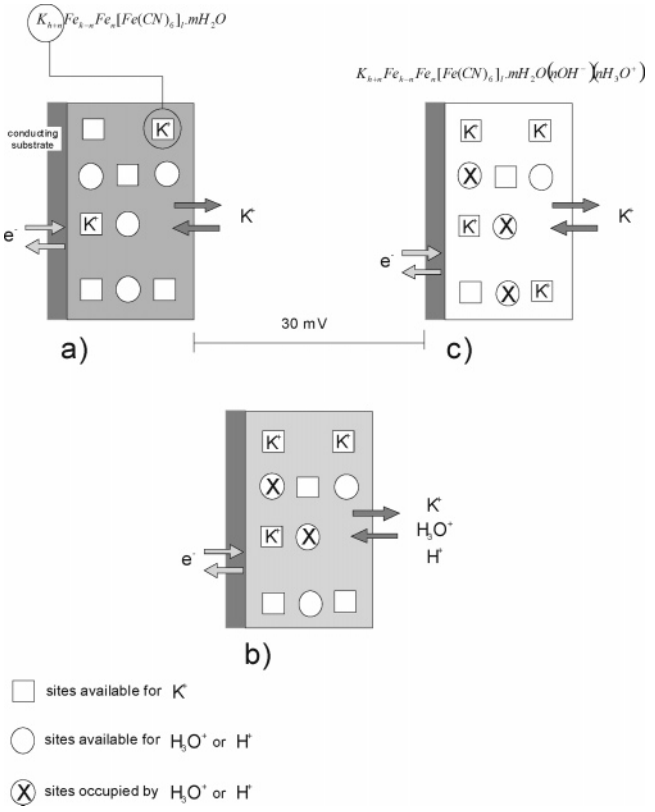

Figure 5. This figure roughly represents the mechanism proposed to describe the observed changeover. It is best understandable if rationalized based on Figure 2. (a) Represents the PB host material in a potential around 0.17 V (transition between zone 1 and zone 3). (b) Indicates the region of 0.17 V up to 0.14 V (zone 3) where effectively the changeover occurs (a difference in terms of potential of only 30 mV). (c) Shows the beginning of zone 2 and the end of zone 3, where a complete different PB host materials (totally changed in terms of properties) is formed due to structural rearrangement or changes (with higher content of K^+ and H_2O clusters).

magnetism properties. In general, the structural changeover observed in magnetic, optic, and electrochemical properties occurs when vacancies are filled up with $(H_2O)_6$ clusters during an in situ compositional variation. In this narrow range of compositional variations, hexacyanoferrates change their properties completely. It is common to associate this region to the exchange of K^+ ions due to PB reduction, but it was shown here that a previous specific K^+ occupation in the compound structure (25% of occupation) activates the occupation of the $(H_2O)_6$ cluster by H^+ and/or H_3O^+ in this region. Consequently, the ionic exchange in such a region is not solely due to the potassium ions. On the contrary, the maximum of the peak is mainly due to an exchange resulting from $(H_2O)_6$ cluster filling. Furthermore, the $(H_2O)_6$ clusters and the structural changes also appear to be the source of the electrolumiscence properties of hexacyanoferrate materials.[3]

It is also important to emphasize that the shape of the peak related to the water compositional variation of the structure, which is identified here as lying in the range 0.14−0.17 V (Figure 2b), is very narrow, indicating the existence of localized electronic/ionic sites and corroborating the mechanism proposed here to explain the changeover. This changeover is also in concordance with the shortening of the Co−ligand bond accompanying the $Co^{II}(HS) \rightarrow Co^{III}(LS)$ transformation in CsCoFe Prussian Blue Derivate proposed by Bleuzen et al.[44] Such geometry changes were already observed in perovskite oxides, where they were imposed by interactions between lanthanide ions and oxo bridges and associated with changes in some physical properties.[45]

The in-depth structural analysis and mechanism involving water composition in hexacyanoferrates are highly relevant to an understanding of the true nature of magnetic ordering in this fundamental molecular-based magnetic material. It is known that the magnetic superexchange interactions between Fe^{3+} and Fe^{2+} metallic electronic sites are mediated by the cyano bridges in hexacyanometallates .[4−6,8,10,12,18,24,31] On the one hand, if spin-containing orbitals of magnetic ions are of the same symmetry, the spins couple antiferromagnetically.[13] On the other hand, if the orbitals are orthogonal, then ferromagnetic coupling occurs. Therefore, if a variation of the Fe^{3+}/Fe^{2+} ratio occurs concomitantly to the introduction of $(H_2O)_6$ clusters, a change in the type, strength, and 3D topology of the magnetic coupling is expected.[13,14] Thus, approaches similar to the one used here can be useful to the study of magnetic coupling as a function of $(H_2O)_6$ cluster density, allowing for the in situ compositional variation of $(H_2O)_6$ and providing details about how $(H_2O)_6$ clusters may interfere in the superexchange interactions.[31]

Conclusion

A changeover within a very narrow potential range of ∼30 mV in hexacyanometallate material was found to be determinant in explaining the strong changes observed in the properties of hexacyanometallates (electrical, optical, and probably magnetic) in this transitional region. A careful and detailed analysis of electrogravimetric techniques (in ac and dc modes) revealed that the potential variation is compensated by interstitial site occupation controlled by K^+ metal alkali atoms. However, it was particularly obvious that, at the changeover point, a specific K^+ occupation in the compound structure activates the occupation of the $(H_2O)_6$ cluster by H^+ and/or H_3O^+ in hexacyanometallate material, confirming the importance of $(H_2O)_6$ clusters in hexacyanometallate-based devices. This approach can be exploited in the future to better understand the mechanisms involved in photomagnetic properties, since $\{Fe(CN)_6\}$ vacancies filled by $\{(H_2O)_6\}$ are a prerequisite for the existence of these properties.[29,31] The approach described here is also important to shed light on the mechanism involved in electrochemical tunable magnetic phase transition.[1]

Acknowledgment. This work was supported by FEDER-CICyT Project CTQ 2004-08026/BQV. D.G.-R. acknowledges a fellowship from the Generalitat Valenciana, Postdoctoral Program. P.R.B. acknowledges the São Paulo state research funding agency (FAPESP) for financing Project No. 02/06693-3. J.J.G.-J. acknowledges his position in the Ramon y Cajal Program (Spanish Ministry Office of Education and Science). We appreciate the very useful discussions with Nuria Pastor-Navarro.

JA066982A

(44) Bleuzen, A.; Escax Virgine Ferrier, A.; Villain, F.; Verdaguer, M.; Münsch, P.; Itié, J. P. *Angew. Chem., Int. Ed.* **2004**, *43*, 3728.
(45) Lacorre, P.; Torrance, J. B.; Pannetier, J.; Nazzal, A.; Wang, P. W.; Huang, T. C. J. *Solid State Chem.* **1991**, *91*, 225.